Command Governor-Based Adaptive Control of an Autonomous Helicopter

Daniel Magree,* Tansel Yucelen,† and Eric N. Johnson‡
Georgia Institute of Technology, Atlanta, GA 30332-0150, USA

This paper presents an application of a recently developed command governor-based adaptive control framework to a high-fidelity autonomous helicopter model. This framework is based on an adaptive controller, but the proposed command governor adjusts the trajectories of a given command in order to follow an ideal reference system (capturing a desired closed-loop system behavior) both in transient-time and steady-state without resorting to high-gain learning rates in the adaptation (update) law. The high-fidelity autonomous helicopter is a six rigid body degree of freedom model, with additional engine, fuel and rotor dynamics. Non-ideal attributes of physical systems such as model uncertainty, sensor noise, and actuator dynamics are modeled to evaluate the command governor controller in realistic conditions. The proposed command governor adaptive control framework is shown to reduce attitude error with respect to a standard adaptive control scheme during vehicle maneuvers.

I. Introduction

Numerous adaptive control methodologies have been proposed in the past decades that deal with adaptive stabilization and command following of uncertain dynamical systems (see, for example, Refs. 1–8 and references therein). Most of these approaches have averted the problem of high-gain control with the notable exceptions including Refs. 7, 8. Specifically, Refs. 7, 8 require the knowledge of a conservative upper bound on the unknown constant weights appearing in their uncertainty parametrization in order to design their controllers to achieve predictable closed-loop transient and steady-state system performance. While this conservative upper bound can be available for some specific applications, the actual upper bound may exceed its conservative estimate, for example, when an aircraft undergoes a sudden change in dynamics, such as might be due to reconfiguration, deployment of a payload, docking, or structural damage. In such circumstances, the transient and steady-state system performance of these controllers are no longer guaranteed, since it is not possible to redesign these adaptive controllers online with the new conservative upper bound. Furthermore, the system performance of these adaptive controllers in the presence of large system uncertainties may not be satisfactory as well, since both controllers converge to standard adaptive controllers as this upper bound on the unknown constant weights becomes arbitrarily large. Therefore it is of practical importance to achieve predictable performance without requiring the knowledge of an upper bound or resorting to a high gain controller.

A novel command governor architecture was constructed in Ref. 9 to address the problem of obtaining predictable transient and steady-state system response with adaptive controllers for uncertain dynamical

*Graduate Research Assistant, School of Aerospace Engineering, dmagree@gatech.edu.
†Research Engineer, School of Aerospace Engineering, tansel.yucelen@ae.gatech.edu.
‡Associate Professor, School of Aerospace Engineering, eric.johnson@ae.gatech.edu.

systems without *a priori* knowledge of this conservative upper bound and without requiring high-gain learning rates. Specifically, the proposed command governor is a linear dynamical system which adjusts the trajectories of a given command in order to follow an ideal reference system (capturing a desired closed-loop system behavior) both in transient-time and steady-state. That is, by choosing the design parameter of the command governor, the controlled uncertain dynamical system approximates a Hurwitz linear time-invariant dynamical system with $\mathcal{L}_\infty$ input-output signals.

In this paper, we present an application of the command governor-based adaptive control framework to an autonomous helicopter. This helicopter is simulated in the Georgia Tech unmanned aerial vehicle simulation tool (GUST). The GUST software package that combines a high-fidelity vehicle and environment model, onboard flight control software, and ground station software. GUST may be operated in hardware in the loop (HITL) mode or software in the loop (SITL) mode. In HITL mode, the flight control software and ground station interface with physical sensors, actuators, and communication links. In SITL mode, the flight control software and ground station interface with the vehicle model and simulated communication links. This design ensures that the same flight control software is used in simulation and in flight. The vehicle model is a six rigid body degree of freedom model with additional engine, fuel, and rotor dynamics. The vehicle model simulates sensor noise, delay, location, orientation, and actuator dynamics and saturation. The vehicle model can also simulate external disturbances such as turbulence and wind. The results in the paper are from the SITL testing.

The notation used in this paper is fairly standard. Specifically, $\mathbb{R}$ denotes the set of real numbers, $\mathbb{R}^n$ denotes the set of $n \times 1$ real column vectors, $\mathbb{R}^{n\times m}$ denotes the set of $n \times m$ real matrices, $\mathbb{R}_+$ (resp., $\overline{\mathbb{R}}_+$) denotes the set of positive (resp., nonnegative-definite) real numbers, $\mathbb{R}_+^{n\times n}$ (resp., $\overline{\mathbb{R}}_+^{n\times n}$) denotes the set of $n\times n$ positive-definite (resp., nonnegative-definite) real matrices, $\mathbb{S}^{n\times n}$ denotes the set of $n\times n$ symmetric real matrices, $(\cdot)^{\mathrm{T}}$ denotes transpose, $(\cdot)^{-1}$ denotes inverse, and "$\triangleq$" denotes equality by definition. In addition, we write $\lambda_{\min}(A)$ (resp., $\lambda_{\max}(A)$) for the minimum (resp., maximum) eigenvalue of the Hermitian matrix A, $\det(A)$ for the determinant of the Hermitian matrix A, $\mathrm{tr}(\cdot)$ for the trace operator, A^{L} for the left inverse $(A^{\mathrm{T}}A)^+A^{\mathrm{T}}$ of $A \in \mathbb{R}^{n\times m}$, P_{A} for the projection matrix AA^{L} of $A \in \mathbb{R}^{n\times m}$, $\|\cdot\|_2$ for the Euclidian norm, $\|\cdot\|_\infty$ for the infinity norm, and $\|\cdot\|_{\mathrm{F}}$ for the Frobenius matrix norm.

II. Preliminaries

We begin by presenting a standard model reference adaptive control problem. Specifically, consider the nonlinear uncertain dynamical system given by

$$\dot{x}(t) \quad = \quad Ax(t) + B\big[u(t) + \delta(x(t))\big], \quad x(0) = x_0, \quad t \in \overline{\mathbb{R}}_+, \tag{1}$$

where $x(t) \in \mathbb{R}^n$ is the state vector available for feedback, $u(t) \in \mathbb{R}^m$ is the control input, $\delta : \mathbb{R}^n \to \mathbb{R}^m$ is an *uncertainty*, $A \in \mathbb{R}^{n\times n}$ is a known system matrix, and $B \in \mathbb{R}^{n\times m}$ is a known control input matrix such that $\det(B^{\mathrm{T}}B) \neq 0$ and the pair (A, B) is controllable.

Assumption 1. The uncertainty in (1) is parameterized as

$$\delta(x) \quad = \quad W^{\mathrm{T}}\sigma(x), \quad x \in \mathbb{R}^n, \tag{2}$$

where $W \in \mathbb{R}^{s\times m}$ is an *unknown* weight matrix and $\sigma : \mathbb{R}^n \to \mathbb{R}^s$ is a known basis function of the form $\sigma(x) = [\sigma_1(x), \sigma_2(x), \ldots, \sigma_s(x)]^{\mathrm{T}}$.

Next, consider the ideal reference system capturing a desired closed-loop dynamical system performance given by

$$\dot{x}_{\mathrm{r}}(t) \quad = \quad A_{\mathrm{r}}x_{\mathrm{r}}(t) + B_{\mathrm{r}}c(t), \quad x_{\mathrm{r}}(0) = x_{\mathrm{r}0}, \quad t \in \overline{\mathbb{R}}_+, \tag{3}$$

where $x_{\mathrm{r}}(t) \in \mathbb{R}^n$ is the reference state vector, $c(t) \in \mathbb{R}^m$ ia a bounded command for tracking (or $c(t) = 0$ for stabilization), $A_{\mathrm{r}} \in \mathbb{R}^{n\times n}$ is the Hurwitz reference system matrix, and $B_{\mathrm{r}} \in \mathbb{R}^{n\times m}$ is the command input matrix. Also, their exist matrices $K_1 \in \mathbb{R}^{m\times n}$ and $K_2 \in \mathbb{R}^{m\times m}$ such that $A_{\mathrm{r}} = A + BK_1$, $B_{\mathrm{r}} = BK_2$, and $\det(K_2) \neq 0$ hold.

Consider the feedback law

$$u(t) \quad = \quad u_{\mathrm{n}}(t) + u_{\mathrm{a}}(t), \tag{4}$$

where $u_{\mathrm{n}}(t)$ is the nominal feedback control law given by

$$u_{\mathrm{n}}(t) = K_1x(t) + K_2c(t), \tag{5}$$

Using (4) and (5) in (1) subject to Assumption 1 gives

$$\dot{x}(t) = A_{\mathrm{r}}x(t) + B_{\mathrm{r}}c(t) + B\big[u_a(t) + W^{\mathrm{T}}\sigma(x(t))\big]. \tag{6}$$

Next, let the adaptive feedback control law $u_{\mathrm{a}}(t)$ be given by

$$u_{\mathrm{a}}(t) = -\hat{W}^{\mathrm{T}}(t)\sigma(x(t)), \tag{7}$$

where $\hat{W}(t) \in \mathbb{R}^{s\times m}$ is the estimate of W satisfying the weight update law

$$\dot{\hat{W}}(t) \quad = \quad \Gamma\sigma(x(t))e^{\mathrm{T}}(t)PB, \quad \hat{W}(0) = \hat{W}_0, \quad t \in \overline{\mathbb{R}}_+, \tag{8}$$

where $\Gamma \in \mathbb{R}_+^{s\times s} \cap \mathbb{S}^{s\times s}$ is the learning rate matrix, $e(t) \triangleq x(t) - x_{\mathrm{r}}(t)$ is the system error state vector, and $P \in \mathbb{R}_+^{n\times n} \cap \mathbb{S}^{n\times n}$ is a solution of the Lyapunov equation

$$0 = A_{\mathrm{r}}^{\mathrm{T}}P + PA_{\mathrm{r}} + R, \tag{9}$$

where $R \in \mathbb{R}_+^{n\times n} \cap \mathbb{S}^{n\times n}$ can be viewed as an additional learning rate. Note that since A_{r} is Hurwitz, it follows from converse Lyapunov theory[10] that there exists a unique P satisfying (9) for a given R. Now, using (7) in (6) gives

$$\dot{x}(t) = A_{\mathrm{r}}x(t) + B_{\mathrm{r}}c(t) - B\tilde{W}^{\mathrm{T}}(t)\sigma(x(t)). \tag{10}$$

where $\tilde{W}(t) \triangleq \hat{W}(t) - W$ and system error dynamics is given by using (3) and (10)

$$\dot{e}(t) = A_{\mathrm{r}}e(t) - B\tilde{W}^{\mathrm{T}}(t)\sigma(x(t)), \quad e(0) = e_0, \quad t \in \bar{\mathbb{R}}_+. \tag{11}$$

where $e_0 \triangleq x_0 - x_{r0}$. Proofs of Lyapunov stability of the weight matrix $\hat{W}(t)$ and error vector $e(t)$ and the convergence of $e(t) \to 0$ as $t \to \infty$ can be found in reference [9].

Even though the above analysis shows that the state vector $x(t)$ asymptotically converges to the reference state vector $x_{\mathrm{r}}(t)$ (in steady-state), $x(t)$ can be far different from $x_{\mathrm{r}}(t)$ in transient time. High-gain learning rates can be used in (7) in order to achieve fast adaptation and to minimize the distance between $x(t)$ and

$x_{\rm r}(t)$ in transient time. However, update law with high-gain learning rates possibly lead to high-frequency oscillations especially during the transient system response resulting in system instability for real applications[11–13].

III. Command Governor-based Adaptive Control

The recently developed command governor architecture may be applied to a variety of adaptive and non-adaptive control frameworks. This section overviews the command governor architecture[9] applied to the adaptive control problem described in the previous section. Specifically, let the command $c(t)$ be given by

$$c(t) \quad = \quad c_{\rm d}(t) + G\eta(t), \tag{12}$$

where $c_{\rm d}(t) \in \mathbb{R}^m$ is a bounded external command for tracking (or $c_{\rm d}(t) \equiv 0$ for stabilization) and $G\eta(t) \in \mathbb{R}^m$ is the command governor signal with $G \in \mathbb{R}^{m\times n}$ being the matrix defined by

$$G \quad \triangleq \quad K_2^{-1}B^{\rm L} = K_2^{-1}(B^{\rm T}B)^{-1}B^{\rm T}, \tag{13}$$

and $\eta(t) \in \mathbb{R}^n$ being the command governor output generated by

$$\dot{\xi}(t) \quad = \quad -\lambda\xi(t) + \lambda e(t), \quad \xi(0) = 0, \quad t \in \overline{\mathbb{R}}_+, \tag{14}$$

$$\eta(t) \quad = \quad \lambda\xi(t) + \big(A_{\rm r} - \lambda I_n\big)e(t), \tag{15}$$

where $\xi(t) \in \mathbb{R}^n$ is the command governor state vector and $\lambda \in \mathbb{R}_+$ is the command governor gain.

The addition of the command governor signal $G\eta(t)$ to the command for tracking $c_{\rm d}(t)$ in (12) does not change the system error dynamics, and hence, the weight update law (8) for $\hat{W}(t)$ remains the same. In this case, however, (3) and (10) change to

$$\dot{x}_{\rm r}(t) \quad = \quad A_{\rm r}x_{\rm r}(t) + B_{\rm r}c_{\rm d}(t) + P_{\rm B}\eta(t), \tag{16}$$

$$\dot{x}(t) \quad = \quad A_{\rm r}x(t) + B_{\rm r}c_{\rm d}(t) + P_{\rm B}\eta(t) - B\tilde{W}^{\rm T}(t)\sigma(x(t)), \tag{17}$$

where $P_{\rm B} = BB^{\rm L} = B(B^{\rm T}B)^{-1}B^{\rm T}$. Even though this implies the modification of the reference system with the signal $P_{\rm B}\eta(t)$, as we see later, by properly choosing the command governor gain λ it is possible to suppress the effect of $B\tilde{W}^{\rm T}(t)\sigma(x(t))$ in (17) through $P_{\rm B}\eta(t)$.

For the following theorem, we assume that the choice of R in (11) satisfies $R = R_0 + \gamma\lambda I_n$, where $R_0 \in \mathbb{R}_+^{n\times n} \cap \mathbb{S}^{n\times n}$ and $\gamma \in \mathbb{R}_+$ is an arbitrary constant that can be chosen to be sufficiently small. Therefore, this assumption is technical and does not place restrictions on the selection of R. Also, the weight update error dynamics is given by

$$\dot{\tilde{W}}(t) \quad = \quad \Gamma\sigma(x(t))e^{\rm T}(t)PB, \quad \tilde{W}(0) = \tilde{W}_0, \quad t \in \overline{\mathbb{R}}_+, \tag{18}$$

Theorem 1. Consider the nonlinear uncertain dynamical system given by (1) subject to Assumption 1, the reference system given by (3) with the command given by (12), the feedback control law given by

(4) along with (5), (7), and (8), and the command governor given by (14) and (15). Then, the solution $\big(e(t), \tilde{W}(t), \xi(t)\big)$ of the closed-loop dynamical system given by (11), (14), and (18) is Lyapunov stable for all $\big(e_0, \tilde{W}_0, 0\big) \in \mathbb{R}^n \times \mathbb{R}^{s\times m} \times \mathbb{R}^n$ and $t \in \overline{\mathbb{R}}_+$, and $\lim_{t\to\infty} e(t) = 0$, $\lim_{t\to\infty} \xi(t) = 0$, $\lim_{t\to\infty} \eta(t) = 0$, and $\lim_{t\to\infty} \big(c(t) - c_{\rm d}(t)\big) = 0$. For $t \in \overline{\mathbb{R}}_+$, in addition, the system error state vector, the weight update error dynamics, and the command governor dynamics satisfy the transient performance bounds given by

$$\|e(t)\|_{\mathcal{L}_\infty} \leq \Big[\big(\lambda_{\max}(P)\|e_0\|_2^2 + \|\Gamma^{-1}\|_{\rm F}\|\tilde{W}_0\|_{\rm F}^2\big)/\lambda_{\min}(P)\Big]^{\frac{1}{2}}, \tag{19}$$

$$\|\mathrm{vec}(\tilde{W}(t))\|_{\mathcal{L}_\infty} \leq \Big[\big(\lambda_{\max}(P)\|e_0\|_2^2 + \|\Gamma^{-1}\|_{\rm F}\|\tilde{W}_0\|_{\rm F}^2\big)/\lambda_{\min}(\Gamma^{-1})\Big]^{\frac{1}{2}}, \tag{20}$$

$$\|\xi(t)\|_{\mathcal{L}_\infty} \leq \Big[\big(\lambda_{\max}(P)\|e_0\|_2^2 + \|\Gamma^{-1}\|_{\rm F}\|\tilde{W}_0\|_{\rm F}^2\big)/\gamma\Big]^{\frac{1}{2}}. \tag{21}$$

where $\gamma \in \mathbb{R}_+$. If, in addition, command governor gain $\lambda \to \infty$, then $\eta(\cdot) \in \mathcal{L}_\infty$ and (1) approximates

$$\dot{x}(t) = A_{\rm r}x(t) + B_{\rm r}c_{\rm d}(t), \tag{22}$$

$$z(t) = C_{\rm r}x(t), \tag{23}$$

where $A_{\rm r} = A + BK_1$ is Hurwitz, $B_{\rm r} = BK_2$, $C_{\rm r} = I_n$, $c_{\rm d}(\cdot) \in \mathcal{L}_\infty$, and $z(\cdot) \in \mathcal{L}_\infty$.

Proof. See the proofs of Theorems 1 and 2 in Ref. 9.

Theorem 1 highlights not only the stability but also the transient and steady-state performance guarantees of the closed-loop dynamical system given by (11), (14), and (18). Note that it also shows that $\lim_{t\to\infty} \eta(t) = 0$, and hence, the modified reference system in (16) converges to the ideal reference system

$$\dot{x}_{\rm r}(t) = A_{\rm r}x_{\rm r}(t) + B_{\rm r}c_{\rm d}(t), \tag{24}$$

as $t \to \infty$. It is of practical importance to note that the same theorem demonstrates the convergence of the system dynamics to the reference model dynamics as $\lambda \to \infty$. Hence, the learning rate matrix Γ for (8) can be chosen to be sufficiently small. However, it should be also noted that a very high command governor gain λ can amplify the measurement noise which possibly exists in the state error vector of a real physical system.[9] Hence, for real applications, λ should be large enough (and hence, Γ should be small enough) to *approximately* guarantee that (1) behaves as (24) in transient system response, but should not be very large in order to avoid measurement noise amplification.

In physical systems with measurement noise, it is desirable to reduce the transmission of measurement noise while maintaining the tracking benefits of high λ. To accomplish this goal, the command governor output may be modified to make it less sensitive to the high frequency dynamical content despite high values of λ. Specifically, let the modified command be given by

$$c(t) = c_{\rm d}(t) + G\eta_f(t), \tag{25}$$

and let the modified command governor signal, $\eta_f(t)$, be given by the following dynamic equation

$$\dot{\eta}_f(t) = -\kappa\eta_f(t) + \kappa\eta(t), \quad \eta_f(0) = 0, \quad t \in \overline{\mathbb{R}}_+. \tag{26}$$

Note that this system acts as a low-pass filter with cutoff frequency at κ rad/s. It should be noted that the selection of this filter is *not* unique, and it is often desirable to select κ differently depending on the

command governor output direction, i.e.

$$\kappa \triangleq diag\,(\kappa_1, \kappa_2, ..., \kappa_m) \tag{27}$$

The following theorem describes the stability characteristics of the robust command governor architecture, including the transient bounds and in the limit as $\lambda \to \infty$. As in Theorem 1, we assume that the choice of R in (11) satisfies $R = R_0 + \gamma\lambda I_n$.

Theorem 2. Consider the nonlinear uncertain dynamical system given by (1) subject to Assumption 1, the reference system given by (3) with the command given by (25), the feedback control law given by (4) along with (5), (7), and (8), and the command governor given by (14), (15), and (26). Then, the solution $\big(e(t), \tilde{W}(t), \xi(t), \eta_f(t)\big)$ of the closed-loop dynamical system given by (11), (14), (18), and (26) is Lyapunov stable for all $\big(e_0, \tilde{W}_0, 0, 0\big) \in \mathbb{R}^n \times \mathbb{R}^{s\times m} \times \mathbb{R}^n \times \mathbb{R}^m$ and $t \in \overline{\mathbb{R}}_+$, and $\lim_{t\to\infty} e(t) = 0$, $\lim_{t\to\infty} \xi(t) = 0$, $\lim_{t\to\infty} \eta(t) = 0$, $\lim_{t\to\infty} \eta_f(t) = 0$ and $\lim_{t\to\infty} \big(c(t) - c_{\rm d}(t)\big) = 0$. For $t \in \overline{\mathbb{R}}_+$, in addition, the system error state vector, the weight update error dynamics, and the command governor dynamics satisfy the transient performance bounds given by (19), (20), and (21), and

$$\|\eta_f(t)\|_{\mathcal{L}_\infty} \leq \Big[\big(\lambda_{\max}(P)\|e_0\|_2^2 + \|\Gamma^{-1}\|_{\rm F}\|\tilde{W}_0\|_{\rm F}^2\big)/\zeta\Big]^{\frac{1}{2}}, \tag{28}$$

where $\zeta \in \mathbb{R}_+$ is chosen such that $\min\big\{\frac{\lambda_{min}(R_0)}{\kappa\|A_r - \lambda I_n\|_F^2}, \frac{\gamma}{\kappa\lambda}\big\} > \zeta$ holds.

and $\gamma \in \mathbb{R}_+$. If, in addition, command governor gain $\lambda \to \infty$, then $\eta_f(\cdot) \in \mathcal{L}_\infty$ and (1) approximates

$$\dot{x}(t) = A_{\rm r}x(t) + B_{\rm r}c_{\rm d}(t) + P_B\big(\eta_f(t) - \eta(t)\big), \tag{29}$$

$$z(t) = C_{\rm r}x(t), \tag{30}$$

where $A_{\rm r} = A + BK_1$ is Hurwitz, $B_{\rm r} = BK_2$, $C_{\rm r} = I_n$, $P_B = BB^L$, $c_{\rm d}(\cdot) \in \mathcal{L}_\infty$, $z(\cdot) \in \mathcal{L}_\infty$, and $\lim_{t\to\infty} P_B\big(\eta_f(t) - \eta(t)\big) = 0$.

Proof. See the proofs of Theorems 7.1 and Proposition 7.1 in Ref. 14

Theorem 2 shows that the addition of the low-pass filter does not affect the stability properties or the transient performance bounds defined in Theorem 1. Furthermore, Theorem 2 shows that the controlled nonlinear uncertain dynamical system (1) approximates the ideal reference system (22) modified by the term $P_B\big(\eta_f(t) - \eta(t)\big)$, which has the property $\lim_{t\to\infty} P_B\big(\eta_f(t) - \eta(t)\big) = 0$ as $\lambda \to \infty$. For more details, see Ref. 14

A block diagram showing the proposed command governor-based adaptive control architecture is given in Figure 1.

IV. Application to a High-Fidelity Autonomous Helicopter Model

This section describes the implementation of command governor architecture in the Georgia Tech unmanned aerial vehicle simulation tool (GUST). GUST contains a high-fidelity helicopter model developed at the Georgia Tech Unmanned Aerial Vehicle Research Facility (UAVRF) for rapid development and testing of software for all aspects of autonomous vehicle operation. As described in the introduction, GUST has the ability to simulate many non-ideal phenomena including wind and turbulence, nonlinear vehicle dynamics, control actuator dynamics, time delay, and sensor noise to ensure realistic vehicle behavior.

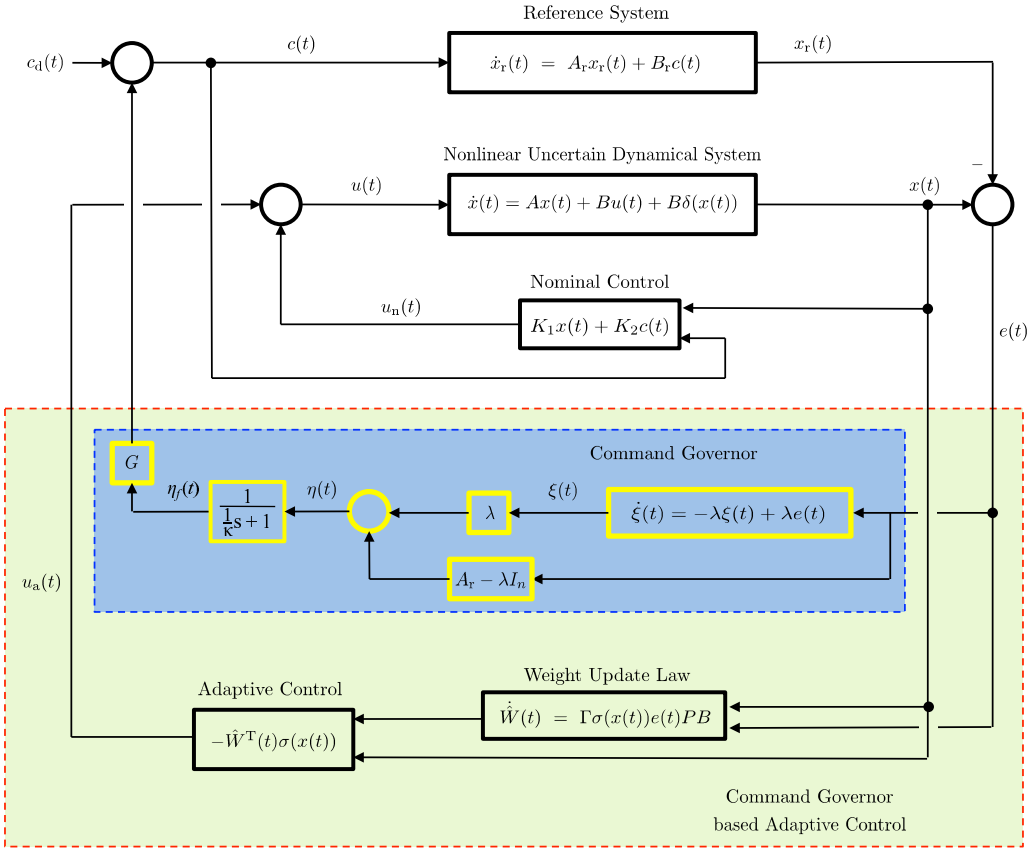

Figure 1. Visualization of the proposed command governor based adaptive control architecture.

The vehicle simulation model used in this paper is that of a Yamaha RMAX helicopter. The baseline control algorithm is a dynamic inversion adaptive controller. The control architecture is separated into an inner attitude loop and outer position loop. Position and velocity commands are fed into the reference model that we wish the controller to track to generate desired acceleration, called a pseudocontrol. The pseudocontrol is then fed into an approximate inversion model to obtain the actuator deflections. The adaptive element cancels the uncertainty, which can be viewed as the difference between the approximate inversion model and the real system dynamics for both inner and the outer loops. For more details on the controller architecture, see Ref. 15.

In the description of the implementation of command governor, pseudocontrol hedging is left out for conciseness, since it is independent of command governor. Details on pseudocontrol hedging can be found in Ref. 15. First, consider the vehicle dynamic model given by

$$\dot{p} = v \tag{31}$$
$$\dot{v} = a(p, v, q, u_f, u_m) \tag{32}$$
$$\dot{q} = \dot{q}(q, \omega) \tag{33}$$
$$\dot{\omega} = \alpha(p, v, q, \omega, u_f, u_m), \tag{34}$$

where $p \in \mathbb{R}^3$ is vehicle postion, $v \in \mathbb{R}^3$ is velocity, $q \in \mathbb{R}^4$ is the attitude quaternion, $\omega \in \mathbb{R}^3$ is angular

velocity. $u_f \in \mathbb{R}$ and $u_m \in \mathbb{R}^3$ are primary force and moment actuators respectively. We may now define the state vector and control vector

$$x \triangleq [p^{\mathrm{T}} v^{\mathrm{T}} q^{\mathrm{T}} \omega^{\mathrm{T}}]^{\mathrm{T}} \tag{35}$$
$$u \triangleq [u_f^{\mathrm{T}} u_m^{\mathrm{T}}]^{\mathrm{T}}. \tag{36}$$

Let the actuator dynamics be given by

$$\dot{u} = \begin{bmatrix} g_f(x, u_f, u_{f_{des}}) \\ g_m(x, u_m, u_{m_{des}}) \end{bmatrix} = g(x, u, u_{des}) \tag{37}$$

where u, u_{des} are the true control input and desired control input, respectively. Models of translational and rotational dynamics are given by

$$a_{des} = \hat{a}(x, q_{des}, u_{fdes}) \tag{38}$$
$$\alpha_{des} = \hat{\alpha}(x, u_{mdes}) \tag{39}$$

where q_{des} is the attitude command from the outer control loop. Inverting the models give actuator positions necessary to achieve desired accelerations.

$$\begin{bmatrix} q_{des} \\ u_{fdes} \end{bmatrix} = \hat{a}^{-1}(x, a_{des}) \tag{40}$$
$$u_{mdes} = \hat{\alpha}^{-1}(x, \alpha_{des}) \tag{41}$$

Combining equations (32) and (38) and equations (34) and (39),

$$\dot{v} = a(x, u) + a_{des} - \hat{a}(x, q_{des}, u_{fdes}) \tag{42}$$
$$\dot{\omega} = \alpha(x, u) + \alpha_{des} - \hat{\alpha}(x, u_{mdes}) \tag{43}$$

Now define error between achieved pseudocontrol and true acceleration as

$$\bar{\Delta}_a \triangleq a(x, u) - \hat{a}(x, q_{des}, u_{fdes}) \tag{44}$$
$$\bar{\Delta}_\alpha \triangleq \alpha(x, u) - \hat{\alpha}(x, u_{mdes}) \tag{45}$$

Then

$$\dot{v} = a_{des} + \bar{\Delta}_a \tag{46}$$
$$\dot{\omega} = a_{des} + \bar{\Delta}_\alpha \tag{47}$$

Now, define pseudocontrols

$$a_{des} = a_c + a_{pd} - \bar{a}_{ad} \tag{48}$$
$$\alpha_{des} = \alpha_c + \alpha_{pd} - \bar{\alpha}_{ad}. \tag{49}$$

Command governor modification is applied to the inner loop reference model by including a new angular acceleration term α_{cg} in the design of the reference model acceleration, α_{cr}

$$a_c = a_c(p_r, v_r, p_c, v_c) \tag{50}$$
$$\alpha_c = \alpha_{cd}(q_r, \omega_r, q_c, \omega_c) + \alpha_{cg}. \tag{51}$$

The full reference model dynamics are then given by

$$\begin{aligned} \dot{p_r} &= v_r && (52)\\ \dot{v_r} &= a_c(p_r, v_r, p_c, v_c) && (53)\\ \dot{q_r} &= \dot{q_r}(q_r, \omega_r) && (54)\\ \dot{\omega_r} &= \alpha_{cd}(q_r, \omega_r, q_c, \omega_c) + \alpha_{cg}. && (55) \end{aligned}$$

where subscript r indicates a reference model state and subscript c indicates a command.

Now, define error state vector

$$e' = \begin{bmatrix} p_r - p \\ v_r - v \\ Q(q_r, q) \\ \omega_r - \omega \end{bmatrix} = \begin{bmatrix} e_1 \\ e_2 \\ e_3 \\ e_4 \end{bmatrix} \tag{56}$$

Where $Q(\cdot,\cdot) : \mathbb{R}^4 \times \mathbb{R}^4 \to \mathbb{R}^3$ gives the three component error vector between quaternions.[15] Then

$$\dot{e}' = \begin{bmatrix} v_r - v \\ \dot{v}_r - \dot{v} \\ \omega_r - \omega \\ \dot{\omega}_r - \dot{\omega} \end{bmatrix} \tag{57}$$

Consider $\dot{e}_4$

$$\begin{aligned} \dot{e}_4 &= \dot{\omega}_r - \dot{\omega} && (58)\\ &= \alpha_{cd} + \alpha_{cg} - \alpha_{des} - \bar{\Delta}_\alpha && (59)\\ &= \alpha_{cd} + \alpha_{cg} - \alpha_{cd} + \alpha_{cg} - \alpha_{pd} + \bar{\alpha}_{ad} - \bar{\Delta}_\alpha && (60)\\ &= -\alpha_{pd} + \bar{\alpha}_{ad} - \bar{\Delta}_\alpha. && (61)\\ & && (62) \end{aligned}$$

Similarly $\dot{e}_1$, $\dot{e}_2$, and $\dot{e}_3$ can also be found. Combining terms, we can write the error dynamics as

$$\dot{e}' = A_r e' + B_r \left(\bar{\Delta} + \nu_{ad}\right) \tag{63}$$

$$A_r = \begin{bmatrix} 0 & I & 0 & 0 \\ -R_p & -R_d & 0 & 0 \\ 0 & 0 & 0 & I \\ 0 & 0 & -K_p & -K_d \end{bmatrix}, \quad B_r = \begin{bmatrix} 0 & 0 \\ I & 0 \\ 0 & 0 \\ 0 & I \end{bmatrix}, \quad \bar{\Delta} = \begin{bmatrix} \bar{\Delta}_a \\ \bar{\Delta}_\alpha \end{bmatrix}, \quad \nu_{ad} = \begin{bmatrix} \bar{a}_{ad} \\ \bar{\alpha}_{ad} \end{bmatrix} \tag{64}$$

$$\tag{65}$$

Therefore, the addition of a command governor signal does not affect the error dynamics, as before. Now dynamic model $\hat{\alpha}$ is chosen to be linear, as follows

$$\alpha_{des} = \hat{\alpha} = \hat{A}_1 v_b + \hat{A}_2 \omega_b + B u_{mdes} \tag{66}$$

where $\hat{A}_1$ and $\hat{A}_2$ are linearized dynamics, and v_b and ω_b are body frame velocity and angular velocity. Inverting, we get

$$u_{mdes} = B^{-1}\left(\alpha_{des} - \hat{A}_1 v_b - \hat{A}_2 \omega_b\right) \tag{67}$$

Finally, we have the tools to determine the command governor signal α_{cg}. Since we are applying the command governor control to the attitude dynamics, we need only consider the attitude dynamics error states. Furthermore, due to the uncoupled nature of the command governor dynamics and the low-pass filter dynamics, we need only consider a 3-state command governor system corresponding to the angular acceleration. To see why this is so, recall that α_{cg} corresponds to the command governor contribution to the plant and model dynamics, and, as such, corresponds to $P_B\eta(t)$ in equations (16) and (17). The control matrix B for the attitude dynamics is defined as

$$B = \begin{bmatrix} 0 \\ I_3 \end{bmatrix} \tag{68}$$

Then

$$P_B = B\big(B^{\mathrm{T}}B\big)^{-1}B^{\mathrm{T}} = \begin{bmatrix} 0 & 0 \\ 0 & I_3 \end{bmatrix} \tag{69}$$

Therefore, only angular acceleration terms remain. The 6-state command governor dynamics, given by

$$\dot{\bar{\xi}}(t) = -\lambda\bar{\xi}(t) - \lambda\begin{bmatrix} e_3(t) \\ e_4(t) \end{bmatrix}, \quad \bar{\xi}(0) = 0, \quad t \in \overline{\mathbb{R}}_+, \tag{70}$$

$$\bar{\eta}(t) = \lambda\bar{\xi}(t) - \left(\begin{bmatrix} 0 & I_3 \\ -K_p & -K_d \end{bmatrix} - \lambda I_6\right)\begin{bmatrix} e_3(t) \\ e_4(t) \end{bmatrix}, \tag{71}$$

$$\dot{\bar{\eta}}_f(t) = -\kappa\bar{\eta}_f(t) + \kappa\bar{\eta}(t), \quad \bar{\eta}_f(0) = 0, \quad t \in \overline{\mathbb{R}}_+, \tag{72}$$

$$\alpha_{cg} = P_B\bar{\eta}_f(t), \tag{73}$$

may be reduced to a 3-state system,

$$\dot{\xi}(t) = -\lambda\xi(t) - \lambda e_4(t) \quad \xi(0) = 0, \quad t \in \overline{\mathbb{R}}_+, \tag{74}$$

$$\eta(t) = \lambda\xi(t) + K_p e_3(t) + (K_d + \lambda I_3)\, e_4(t) \tag{75}$$

$$\dot{\eta}_f(t) = -\kappa\eta_f(t) + \kappa\eta(t), \quad \eta_f(0) = 0, \quad t \in \overline{\mathbb{R}}_+, \tag{76}$$

$$\alpha_{cg} = \eta(t) \tag{77}$$

where $\bar{\eta}(t), \bar{\eta}_f(t), \bar{\xi}(t) \in \mathbb{R}^6$, and $\eta(t), \eta_f(t), \xi(t) \in \mathbb{R}^3$ and are equivalent to the last three states of their barred counterparts. Note the differences in sign between equations (70) and (71) and equations (14) and (15) is due to the different definitions of e' and e.

V. Simulation Results

Values for the matrices in the dynamic model and reference model are chosen as in Ref. 15 for the standard controller. The time delay from controller to actuator output was set to zero; however, other actuator dynamics such as position and rate saturation were modeled.

Figures 2 and 3 presents the results of a 10ft shaped translation command in the longitudinal direction. For this result, full state feedback without sensor noise was provided to the controller. For the command governor controller, command governor gain λ was chosen to be 1, and no filtering was applied to the command governor output. Figure 2 compares the attitude error of the standard controller and command governor. It can be seen that the command governor reduces the maximum and minimum of the error and smooths the response overall. Figure 3 compares the controller output of the standard controller and the command governor. The command governor controller output is reasonable throughout the maneuver.

The second result illustrates the effect of the low-pass filter in the presence of measurement noise. For this result, the simulation was run with sensor models in the loop, and an extended Kalman filter provided state feedback to the controllers. Again, a 10ft shaped translation was commanded in the longitudinal direction. For the command governor controller, command governor gain λ was chosen to be 10, and filter gain κ was chosen to be 2. Figure 4 compares the attitude error of the standard controller and command governor. It can be seen that the command governor reduces the error over the course of the maneuver. Figure 5 compares the controller output of the standard controller and the command governor. Again, no ill effects can be seen in the command governor controller output.

VI. Conclusion

In this paper, we present an application of the command governor-based adaptive control framework to a high-fidelity autonomous helicopter model. We first present the key theorem of command governor-based adaptive control. Next, we present the implementation of the controller on the inner attitude loop of an existing model inversion adaptive controller. Finally we compare standard and command governor controller simulation results of the autonomous helicopter during translation maneuvers. The command governor controller improved tracking in all cases, and kept control inputs within reasonable limits.

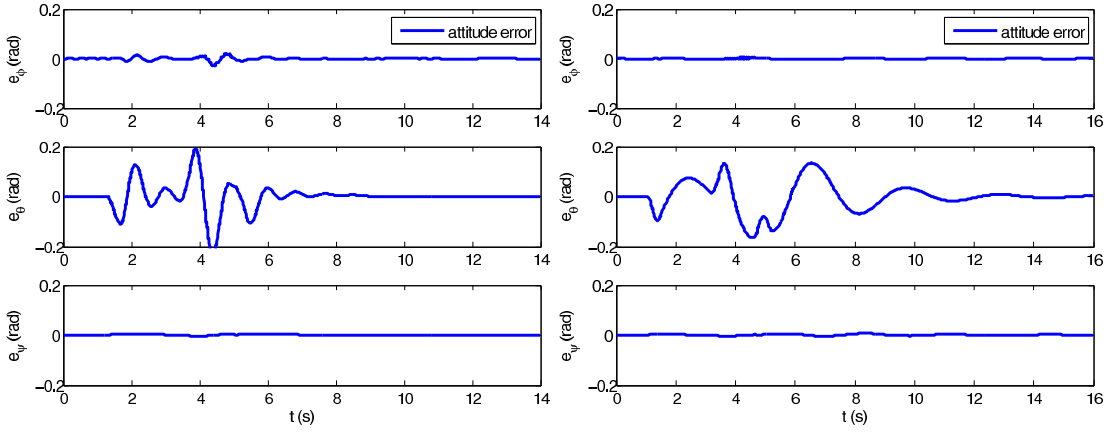

Figure 2. Attitude tracking error for standard adaptive control (left) and command governor-based adaptive control (right) for a 10ft longitudinal command with state feedback. In the command governor case, $\lambda = 1$ and command governor output was not filtered.

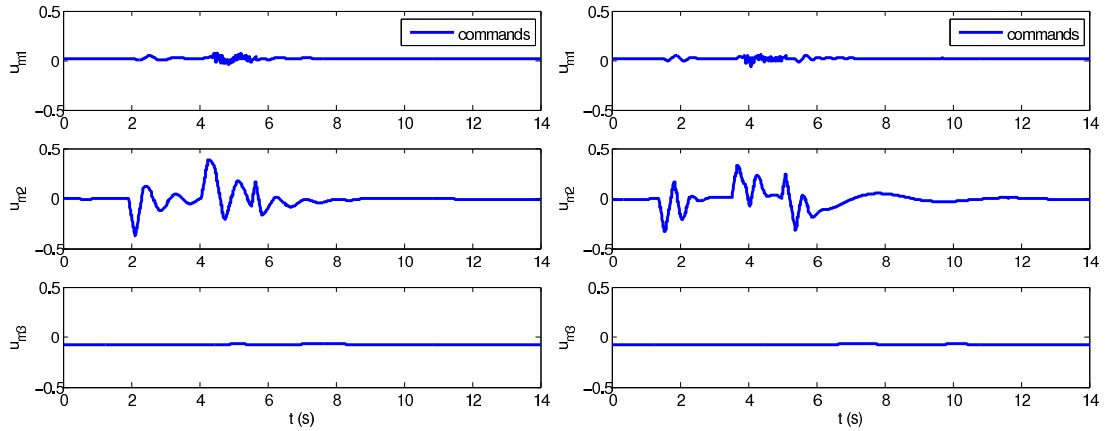

Figure 3. Controller output for standard adaptive control (left) and command governor-based adaptive control (right) for a 10ft longitudinal command with state feedback. In the command governor case, $\lambda = 1$ and command governor output was not filtered.

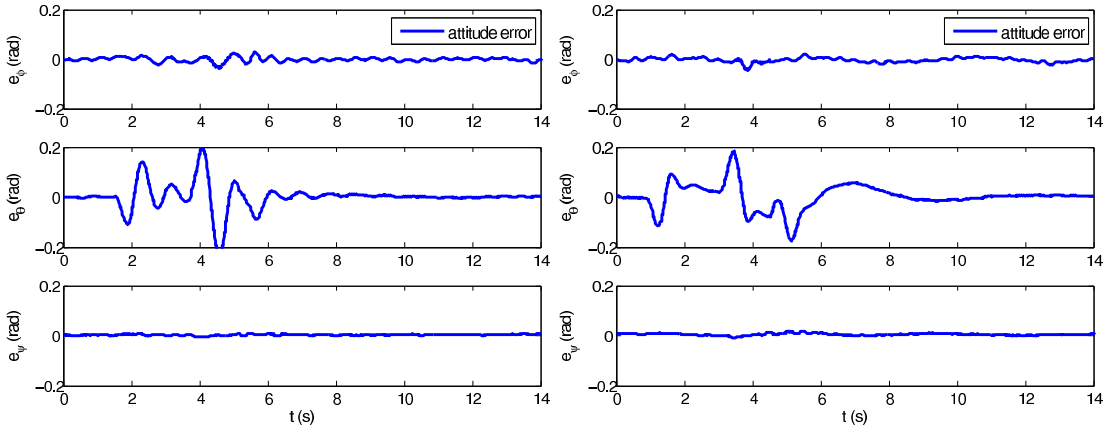

Figure 4. Attitude tracking error for standard adaptive control (left) and command governor-based adaptive control (right) for a 10ft longitudinal command with output feedback. In the command governor case, $\lambda = 10$ and $\kappa = 2$.

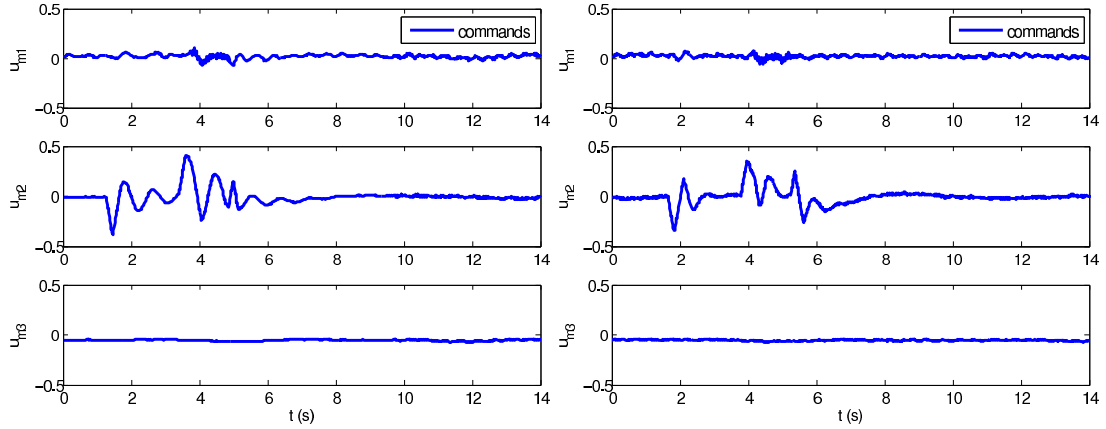

Figure 5. Controller output for standard adaptive control (left) and command governor-based adaptive control (right) for a 10ft longitudinal command with output feedback. In the command governor case, $\lambda = 10$ and $\kappa = 2$

References

[1]P. Ioannou and P. Kokotovic, "Instability analysis and improvement of robustness of adaptive control," *Automatica*, vol. 20, no. 5, pp. 583–594, 1984.

[2]K. S. Narendra and A. M. Annaswamy, "A new adaptive law for robust adaptation without persistent excitation," *IEEE Transactions on Automatic Control*, vol. 32, no. 2, pp. 134–145, 1987.

[3]K. J. Astrom and B. Wittenmark, *Adaptive Control*. Reading, MA: Addison-Wesley, 1989.

[4]F. L. Lewis, A. Yesildirek, and K. Liu, "Multilayer neural-net robot controller with guaranteed tracking performance," *IEEE Transactions on Neural Networks*, vol. 7, pp. 388–399, 1996.

[5]G. Chowdhary and E. N. Johnson, "Theory and flight test validation of a concurrent learning adaptive controller," *AIAA J. Guid. Contr. Dyn.*, vol. 34, pp. 592–607, 2010.

[6]T. Yucelen and A. J. Calise, "Derivative-free model reference adaptive control," *AIAA Journal of Guidance, Control, and Dynamics*, vol. 34, pp. 933–950, 2011.

[7]C. Cao and N. Hovakimyan, "Design and analysis of a novel $\mathcal{L}_1$ adaptive control architecture with guaranteed transient performance," *IEEE Transactions on Automatic Control*, vol. 53, pp. 589–591, 2008.

[8]T. Yucelen and W. M. Haddad, "A robust adaptive control architecture for disturbance rejection and uncertainty suppression with $\mathcal{L}_\infty$ transient and steady-state performance guarantees," *International Journal of Adaptive Control and Signal Processing* (submitted).

[9]T. Yucelen and E. N. Johnson, "Command governor-based adaptive control," *Proc. AIAA Guid., Navig., and Contr. Conf.*, 2012.

[10]W. M. Haddad and V. Chellaboina, *Nonlinear Dynamical Systems and Control. A Lyapunov-Based Approach*. Princeton, NJ: Princeton University Press, 2008.

[11]C. E. Rohrs, L. S. Valavani, M. Athans, and G. Stein, "Robustness of continuous-time adaptive control algorithms in the presence of unmodeled dynamics," *IEEE Transactions on Automatic Control*, vol. 30, pp. 881–889, 1985.

[12]T. Yucelen and A. J. Calise, "Kalman filter modification in adaptive control," *AIAA Journal of Guidance, Control, and Dynamics*, vol. 33, pp. 426–439, 2010.

[13]N. Hovakimyan, C. Cao, E. Kharisov, E. Xargay, and I. M. Gregory, "$\mathcal{L}_1$ adaptive control for safety-critical systems," *IEEE Control Systems Magazine*, vol. 31, pp. 54–104, 2011.

[14]T. Yucelen and E. N. Johnson, "A novel command governor architecture for transient response shaping," *IEEE Transactions on Automatic Control*, (submitted).

[15]E. N. Johnson and S. K. Kannan, "Adaptive trajectory control for autonomous helicopters," *AIAA Guid. Contr. Dyn.*, vol. 28, pp. 524–538, 2005.